Cement and Concrete Research 40 (2010) 302–312

Contents lists available at ScienceDirect

Cement and Concrete Research

journal homepage: http://ees.elsevier.com/CEMCON/default.asp

Prediction of time dependent chloride transport in concrete structures exposed to a marine environment

Seung-Woo Pack, Min-Sun Jung, Ha-Won Song, Sang-Hyo Kim, Ki Yong Ann *

School of Civil and Environmental Engineering, Yonsei University, Seoul 120-749, Republic of Korea

ARTICLE INFO

Article history:
Received 19 July 2007
Accepted 25 September 2009

Keywords:
Chloride (D)
Diffusion (C)
Portland cement (D)
Granulated blast-furnace slag (D)

ABSTRACT

A survey of 11 concrete bridges located in a marine environment at 0.65–48.65 years was examined in terms of chloride transport. As a result, the apparent diffusion coefficient (D) and the surface chloride concentration (C_S) are time dependent; the D exponentially decreased with time and the C_S increased in the form of a logarithm function to time. Using these data, governing equations for the D and C_S were derived to predict the chloride transport in a long term. The time dependent model indicated the higher chloride ingresses in ordinary Portland cement (OPC) concrete than the time independent model, due to a build-up of the C_S with time, but ground granulated blast furnace slag (GGBS) concrete indicated a similar range of the chloride ingresses, due to the rapid decrease in the D. To ensure the accuracy of the model that the present study suggested, the fitted model was compared to the well known model of the LIFE 365 together with a chloride profile obtained from an in-situ examination. Then it was found that the model in the present study well predicted the rate of chloride transport, while the LIFE 365 indicated a poor description of the chloride ingress in a long term, due to a constant C_S and an overwhelming rapid decrease in the D.

1. Introduction

Reinforcing steel in concrete is regarded as being protected from active corrosion by a microscopically thin layer of iron oxide, a "passive film" of γ-$Fe_2O_3 \cdot H_2O$ [1]. The supplementary precipitated hydration products form an inhibitive layer on the steel surface, stabilizing the pH of the pore solution to buffer aggressive ions [2]. Notwithstanding, chloride ions can usually corrode the steel embedment in a chloride environment, when a continuous supply of chloride ions to the steel embedment reaches a certain threshold level. Chloride ions are generally present in concrete by penetration of external chloride into concrete. In service, chloride ions are commonly derived from marine environments or from exposure to deicing salts. In marine environments, the failure of bridge decks [3,4], and significant corrosion in building [5] and jetty structures [6] are notable examples of deterioration from external chlorides. The use of deicing salts has also resulted in widespread corrosion problems with bridge decks [7].

Hence, the assessment/prediction of chloride-induced corrosion has received increasing attention, because of its widespread occurrence and the high cost of repair. In the majority of previous studies, a conservative chloride threshold value such as 0.2 [8] or 0.4% [9] by weight of cement has been used to predict the corrosion risk. For chloride transport, Fick's 2nd law is often used to predict chloride penetration in terms of diffusion [10], because of its convenient and easy calculation with constant values of the apparent diffusion coefficient (D) and surface chloride concentration (C_S), which are in fact dependent on concrete mix proportion and degree of contact to a salt environment (e.g. submerged, tidal, splash and aerated zones in a marine environment) [11]. A development of the pore structure with time has been currently considered in assessing the rate of chloride transport; the diffusivity decreases with time [12–14]. Due to the hypothesis that chloride ions and surface concrete make a chemical equilibrium in the form of di-electric layer, the time dependency of the C_S has been ignored in conventional chloride transport model, so that a constant value of the C_S has been widely used in modelling chloride transport in concrete [13,15]. A build-up of the C_S has been taken into account, only when concrete structures are exposed to a marine atmospheric condition [16,17]. It was, however, observed in a survey on in-situ that a build-up of the C_S occurs, even when concretes are exposed to direct contact to seawater such as in tidal/splash zones [18].

The present study examined 11 concrete bridges located in the West Sea side of Korea exposed to the tidal zone, and data on the D and C_S were obtained. These data were fitted as a function of time, and used in a basic model to predict chloride profiles and the corrosion risk. The characteristic of a C_S build-up was considered in solving Fick's 2nd law and the time dependency of the diffusivity was subsequently applied for the solution on the rate of the chloride ingress in concrete.

2. Time dependency of chloride transport

2.1. Background

Concrete consists of a graded mix of aggregate particles in a cement matrix. The aggregates inside a concrete usually have negligible permeability and therefore have little effect on the transport of chloride through

* Corresponding author. Tel.: +82 2 2123 2806; fax: +82 2 364 5300.
E-mail address: k.ann@yonsei.ac.kr (K.Y. Ann).

0008-8846/$ – see front matter © 2009 Elsevier Ltd. All rights reserved.
doi:10.1016/j.cemconres.2009.09.023

concrete. Hence the rate of transport in a concrete is largely dependent on the characteristics of the cement paste, which may include its binder type, porosity and pore size distribution, primarily controlled by its water–cement ratio (W/C). There are a number of mechanisms by which chloride transport can take place in concrete: diffusion, sorption, capillary suction, migration and wick action. Of them, diffusion takes place under the influence of a concentration gradient, which mainly drives the transport of chloride ions in concretes exposed to a direct contact to seawater, for example, submerged, tidal and splash zones, where the moisture condition of the concrete is stable.

Fick's 2nd law, modelling the diffusion of unreactive species (i.e. chloride ions) into a semi-infinite medium (i.e. concrete), is commonly used to describe chloride ion diffusion in concrete as given in Eq. (1). Theoretically, the D can be calculated by measuring the concentration of the C_S and the concentration of chloride ions $C(x, t)$ at the depth x and the exposure duration t.

$$C(x,t) = C_S\left(1-\mathrm{erf}\frac{x}{2\sqrt{Dt}}\right) \quad (1)$$

where, erf is error function. Capillary pores are the most significant means of transport of ions if they are interconnected and filled with pore solution. Their size ranges up to 3–5 μm in diameter [19]. The rate of transport via capillary pores mainly depends on the volume fraction and connectivity of the pores, which can be determined by W/C, cement content, cement fineness, binder type and degree of hydration. For example, low W/C, good curing and replacement with fine pozzolanic materials will result in the capillary pores blocked with gel and thus reduced permeability to water-containing aggressive ions such as chlorides. The importance of W/C and the fineness of binder were previously addressed in the standard specification of concrete structures [20]. Also, the effect of binder on chloride transport has been reported in previous studies that the decrease in the diffusivity for pulverized fuel ash (PFA), ground granulated blast furnace slag (GGBS) or silica fume (SF) concretes generally arises from a refinement of pore structure [15,21,22]. However, the chemical activity between chloride ions and cement (chloride binding) and the change of the pore structure due to hydration are time dependent, as being different from the assumption on unreactive concrete media. It has been reported that the higher chloride binding capacity increased the surface chloride and the rate of chloride diffusion decreased with time. For example, Bentz et al. [23] showed that the D was reduced about 40–69%, when specimens were exposed to seawater for 4 years. The influence of chloride binding by tricalcium aluminate on the transport of chloride was previously addressed [24].

2.2. Time dependency

In this study, 11 concrete bridges exposed to a marine environment were examined to assess the rate of chloride transport, depending on exposure duration and binder type. Among them, 6 bridges at ages ranging from 0.65 to 48.65 years were built in ordinary Portland cement (OPC) concrete as a binder, and the other 5 bridges in GGBS, ranging 20–50% replacement for OPC in binder at 1.35 to 15.5 years. Ground concrete samples from surface concretes were obtained from a pier of the bridges in tidal zone at the time of tide down, as shown in Fig. 1, by drilling and grinding with 2 mm increments up to 50 mm. The preliminary investigation of the environmental condition in terms of temperature and relative humidity showed only a marginal difference of weathering amongst the 11 sampling districts, due to their vicinity. The weathering condition including average monthly temperature and relative humidity (R.H.), and geographic information of sampling are also given in Fig. 1 to consider the environmental condition. The number of sampling for a chloride profile in a bridge structure accounted for 2–6 series. The fluctuation of sea level by the tide ranges 3.45–12.0 m as shown Fig. 1. The chloride content of each sample was determined by acid soluble extraction in a nitric acid solution followed by potentiometric titration against silver nitrite. The chloride concentration of each sample was given in ppm, which was then converted to the percentage by weight of concrete and finally the percentage of chloride by weight of binder, assuming that a uniform distribution of cement through the 50 mm of cover concrete. When the concrete mix proportion is not known, for OPC concretes, a cement content of 350 kg/m^3 and a concrete density of 2300 kg/m^3 were assumed and for GGBS concretes, a binder content (assuming that binder consists of 60% OPC and 40% GGBS) of 400 kg/m^3 and a concrete density of 2200 kg/m^3 respectively, were also assumed

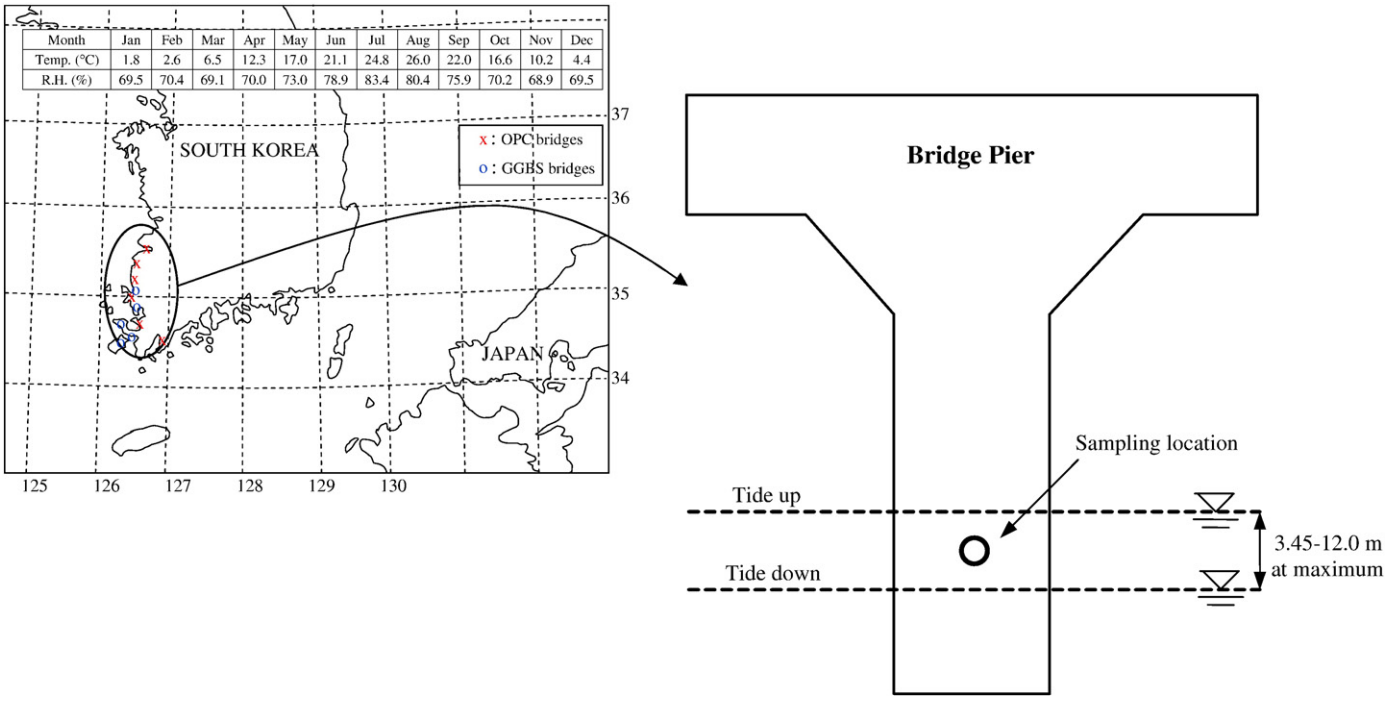

Fig. 1. The location of sampling for chloride profile assessment.

from their strengths, which possibly lead to an error in estimating the rate of chloride transport. The chloride profiles at the time of sampling were also obtained. Then, the D was determined for each specimen by fitting the error function solution to Fick's second law, as given by Eq. (1), for non-steady state diffusion in a semi-infinite medium. A curve is fitted to the chloride profile with the C_S and the D as the independent variables. In the analysis of the chloride profile, the sum of the squared differences between the fitted (theoretical) and the actual data for the chloride content of each sample was minimised by adjusting a regression variable.

Figs. 2 and 3 describe the D and C_S for OPC and GGBS concretes respectively exposed to a tidal zone. Detailed information on chloride transport with time and binder is given in Tables 1 and 2. The best fit curves for the D are expressed as a power function of time, and for the C_S as a logarithm function of time. It is seen that the D for both OPC and GGBS concretes decreased with exposure duration, despite their high deviation at exposure conditions, including different degrees of wave, weathering and presumably segregation of concrete in mixing. The diffusivity for GGBS concretes was always lower than for OPC at a given time and the greater rate of the decrease in the D. The D for OPC initially (at 0.65 years) ranged from 5.53×10^{-12} to 7.89×10^{-12} m^2/s and at the end (at 48.65 years) from 4.47×10^{-12} to 5.55×10^{-12} m^2/s respectively, while for GGBS at 1.35 years from 4.25×10^{-12} to 5.68×10^{-12} m^2/s and at 15.50 years from 1.95×10^{-12} to 3.79×10^{-12} m^2/s respectively. The C_S was also much affected by the exposure duration. The C_S for OPC ranged from 1.85 to 2.21% by weight of cement at 0.65 years and from 2.71 to 3.11% at 48.65 years respectively. For GGBS concretes, the C_S was slightly higher than for OPC, ranging from 1.97 to 2.54% at 1.35 years and from 2.68 to 2.84% at 15.50 years respectively. The t-test was used to statistically ensure the significance between the series of data [25], as given in Appendix A. As a result, a decrease in the D and an increase in the C_S with time were evident until 8.99 years for OPC concretes and until 8.33 years for GGBS concretes, respectively. These results were used to model chloride penetration considering the time dependency of chloride transport in terms of diffusion in the present study.

3. Modelling of chloride transport

It is obvious that consideration of the time dependency of D and C_S at solving Fick's 2nd law can give more informative, accurate prediction of chloride profile, which is not easy to analytically calculate a chloride profile, due to its complexity. In this study, the time dependency of the

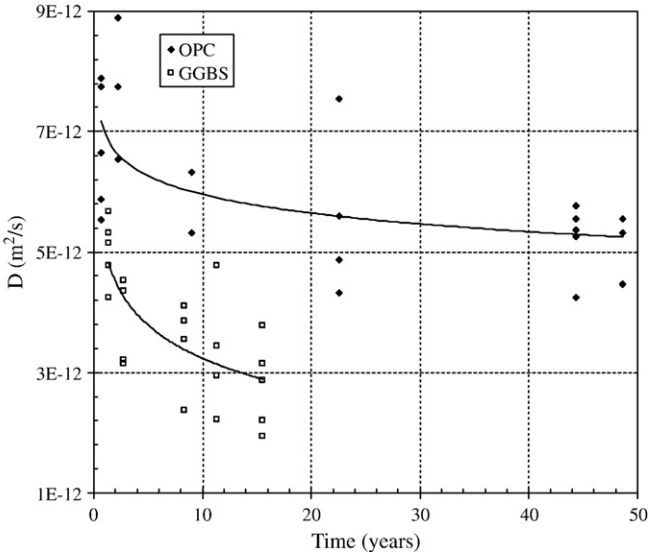

Fig. 2. Apparent diffusion coefficient D measured from 11 concrete bridges of OPC and GGBS concretes exposed to the tidal zone.

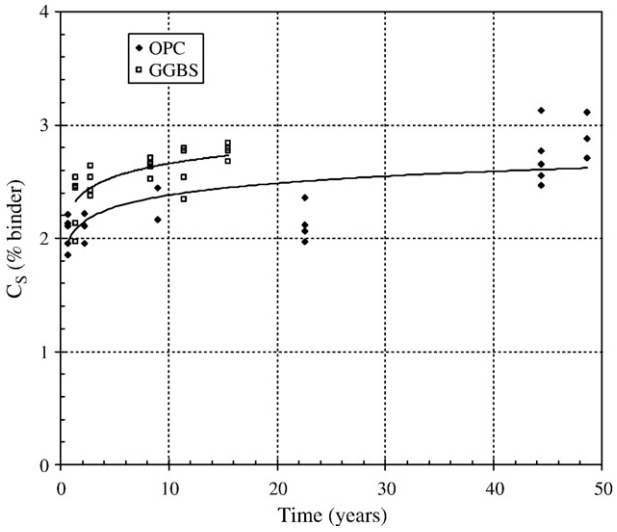

Fig. 3. Concentration of the surface chloride C_S measured from 11 concrete bridges of OPC and GGBS concretes exposed to the tidal zone.

C_S is considered to derive a solution for Fick's 2nd law, and then the time dependent D, obtained by an averaging technique with time is applied to the solution as a variable to calculate the chloride ingress.

3.1. Time dependent diffusion coefficient

The diffusivity often decreases with time, as cement hydration proceeds then to refine the concrete pore structure, thereby letting the connectivity of pores significantly decrease [12,26]. A package program for service life prediction uses a model for determining D in predicting the chloride profile as follows [12].

$$D(t) = D_R\left(\frac{t_R}{t}\right)^m \tag{2}$$

where, $D(t)$ is the diffusion coefficient at time t, D_R is the diffusion coefficient at reference time t_R (i.e. usually 28 days), and m is an age factor. This model is known to fit well for a marine environment, as a change in the pore structure is considered in terms of development of cement hydration [13,17]. However, a direct application of this model for predicting the rate of chloride transport has a defect, since the historic change of the D for a given exposure duration is not considered, which may lead to an erroneous judgment on chloride ingresses and thus the risk of chloride-induced corrosion.

In this study, in order to remedy the defect, the mean value of the D for exposure duration to a marine environment was used to predict a chloride profile. Thus, the mean value was calculated by integrating the definite D for a given exposure duration, and then by dividing the exposure duration, as given in Eq. (3).

$$D_m(t) = \frac{1}{t}\int_0^t D(\tau)\cdot d\tau \tag{3}$$

where $D_m(t)$ is the mean diffusion coefficient for the exposure duration, t. In this study, the time dependency of the D was expressed in power function as seen in Eq. (2) into Eq. (3). Thus the mean D can be obtained as follows:

$$D_m(t) = \frac{D_R}{1-m}\left(\frac{t_R}{t}\right)^m \tag{4}$$

This equation is more useful to solve Fick's 2nd law for a chloride profile, rather than a constant D, since both the time dependency and the hysteretic change of the diffusivity are taken into account [27].

Table 1
The apparent diffusion coefficients and surface chloride contents obtained from in-situ marine environments, and the terms considering time dependency of diffusion for OPC concretes.

Sample number	W/B	Binder content [kg/m^3]	D [$\times 10^{-12}$ m^2/s]	C_S [%, binder]	Time [years]	Terms for time dependent $D_m(t)$			Terms for time dependent $C_S(t)$		
						D_R [$\times 10^{-12}$ m^2/s]	t_R [years]	m	α [%, binder]	β	k [%, binder]
1			7.89	1.85							
2			7.74	2.21							
3	0.38	430	6.65	1.95	0.65						
4			5.53	2.11							
5			5.87	2.13							
6			6.54	1.95							
7	0.39	410	8.89	2.11	2.22						
8			7.74	2.22							
9	0.43	355	6.32	2.44	8.99						
10			5.32	2.16							
11			7.54	2.06		6.74	0.65	0.06	0.26	3.77	1.38
12	0.47	340	5.59	2.36	22.54						
13			4.32	2.12							
14			4.87	1.97		$D_m(t) = \frac{D_R}{1-m}\left(\frac{t_R}{t}\right)^m$			$C_S(t) = \alpha[\ln(\beta t + 1)] + k$		
15			5.55	2.65							
16			5.77	2.77		(Eq. (4))			(Eq. (12))		
17	0.42	360	5.25	3.13	44.36						
18			5.37	2.55							
19			4.25	2.47							
20[a]			5.31	2.71							
21	–	–	5.55	2.88	48.65						
22			4.47	3.11							

[a] Concrete mix proportion has not been known, and thus 350 kg/m^3 of cement, 2300 kg/m^3 of the density of concrete and 0.45 of W/C were assumed in calculating the chloride profile.

3.2. Time dependent surface chloride

Although a previous study suggested that the C_S could increase with time [16], a constant value of the C_S has been often used to model a chloride profile at tidal or splash zone, because of intuitive support that chemical equilibrium at the concrete surface sustain a certain concentration of chloride, when a concrete is subjected to a direct contact with seawater. It is, however, evident that a build-up of the C_S for concrete structures exposed to even seawater was observed in previous surveys [6,18,28]. In this study, the time dependency of the C_S was considered in solving Fick's 2nd law based on the in-situ data (Fig. 3). The chloride content, $C(x, t)$ at a given time t and a depth x can be expressed including the time dependent C_S, which was introduced by utilizing a heat conduction solution in solids [29], as follows.

$$C(x,t) = \int_0^t C_S(\upsilon) \cdot \left(\frac{\partial}{\partial t} F(x, x-\upsilon)\right) d\upsilon \tag{5}$$

Table 2
The apparent diffusion coefficients and surface chloride contents obtained from in-situ marine environments, and the terms considering time dependency of diffusion for GGBS concretes.

Sample number	W/B	Binder content [kg/m^3]		D [$\times 10^{-12}$ m^2/s]	C_S [%, binder]	Time [years]	Terms for time dependent $D_m(t)$			Terms for time dependent $C_S(t)$		
		OPC	GGBS				D_R [$\times 10^{-12}$ m^2/s]	t_R [years]	m	α [%, binder]	β	k [%, binder]
1				4.77	2.46							
2				5.14	2.54							
3	0.38	240	165	5.32	2.13	1.35						
4				4.25	1.97							
5				5.68	2.44							
6				3.22	2.37							
7	0.40	210	200	4.36	2.64	2.77						
8				4.53	2.54							
9				3.15	2.42							
10				3.87	2.65							
11	0.44	182	148	4.11	2.63	8.33	5.03	1.35	0.23	0.18	3.77	2.01
12				2.37	2.71							
13				3.55	2.52		$D_m(t) = \frac{D_R}{1-m}\left(\frac{t_R}{t}\right)^m$			$C_S(t) = \alpha[\ln(\beta t + 1)] + k$		
14				3.45	2.54							
15	0.42	252	168	4.77	2.34	11.36						
16				2.95	2.77		(Eq. (4))			(Eq. (12))		
17				2.22	2.79							
18[a]				2.88	2.77							
19				3.79	2.79							
20	–	–	–	3.15	2.68	15.5						
21				1.95	2.77							
22				2.21	2.84							

[a] Concrete mix proportion has not been provided by the contractor, and thus 400 kg/m^3 of cement, 2200 kg/m^3 of the density of concrete and 0.45 of W/C were assumed in calculating the chloride profile.

Here, the chloride content $F(x,t)$, when concrete is regarded as an infinite medium, is calculated.

$$\begin{aligned} F(x,t) &= 1-\mathrm{erf}\left(\frac{x}{2\sqrt{Dt}}\right) \\ &= 1-\frac{2}{\sqrt{\pi}}\int_0^{\frac{x}{2\sqrt{Dt}}} e^{-\xi^2}d\xi \\ &= \frac{2}{\sqrt{\pi}}\int_{\frac{x}{2\sqrt{Dt}}}^{\infty} e^{-\xi^2}d\xi \end{aligned} \tag{6}$$

Hence, $F(x,t-\lambda)$ can be obtained for an infinite medium.

$$F(x,t-\upsilon) = \frac{2}{\sqrt{\pi}}\int_{\frac{x}{2\sqrt{D(t-\upsilon)}}}^{\infty} e^{-\xi^2}d\xi \tag{7}$$

Thus, the derivative of $F(x,t-\lambda)$ can be calculated as seen in Eq. (8).

$$\begin{aligned} \frac{\partial}{\partial t}F(x,t-\upsilon) &= -\frac{2}{\sqrt{\pi}}\cdot e^{\frac{-x^2}{4D(t-\upsilon)}}\cdot\frac{\partial}{\partial t}\left[\frac{x}{2\sqrt{D(t-\upsilon)}}\right] \\ &= \frac{x}{2\sqrt{\pi D(t-\upsilon)^3}}\cdot e^{\frac{-x^2}{4D(t-\upsilon)}} \end{aligned} \tag{8}$$

Hence, the chloride content $C(x,t)$, as a function of the time t and depth x, is obtained.

$$C(x,t) = \frac{x}{2\sqrt{\pi D}}\int_0^t C_S(\upsilon)\cdot\frac{e^{\frac{-x^2}{4D(t-\upsilon)}}}{\sqrt{(t-\upsilon)^3}}d\upsilon \tag{9}$$

When $\frac{x}{2\sqrt{D(t-\lambda)}}$ is replaced by ω, the chloride content $C(x,t)$ is simply expressed as Eq. (10).

$$C(x,t) = \frac{2}{\sqrt{\pi}}\int_{\frac{x}{2\sqrt{Dt}}}^{\infty} C_S\left(t-\frac{x^2}{4D\omega^2}\right)\cdot e^{-\omega^2}d\omega \tag{10}$$

Eq. (10) was derived from Fick's law by considering C_S variation with time while D remains constant. Although a consideration of the time dependent D could provide the more accurate ingresses of chlorides, the mathematical calculation would be subject to an extreme complexity. Hence, the term D in Eq. (10) was substituted by the time-varying D derived from Eq. (4), but the C_S in Eq. (11), which may still produce a marginal error. The chloride transport can be predicted by the following equation.

$$C(x,t) = \frac{2}{\sqrt{\pi}}\int_{\frac{x}{2\sqrt{D_m(t)t}}}^{\infty} C_S\left(t-\frac{x^2}{4D_m(t)\omega^2}\right)\cdot e^{-\omega^2}d\omega \tag{11}$$

The time dependency of the C_S was observed in the present study as shown in Fig. 3. Hence, a build-up of the C_S was taken into account in calculating a chloride profile using the best fit of a change in the C_S with time [27] from the field data as Eq. (12).

$$C_S(t) = \alpha[\ln(\beta t+1)]+k \tag{12}$$

Here, t is the time of exposure in years and α, β and k are constants obtained from in-situ environments as given in Table 1 for OPC concrete and in Table 2 for GGBS concrete, respectively.

4. Results

4.1. Time dependency of diffusion

In-situ data on the D and the C_S, obtained from 11 reinforced concrete bridges exposed to a tidal zone, was shown in Figs. 2 and 3. The exposure duration for OPC concretes ranged from 0.65 to 48.65 years, while for GGBS concretes from 1.35 to 15.50 years. It is seen that the D decreased with time in the form of an exponential function, irrespective of binder, which may be attributed to a further hydration of cement, leading to a lower pore network. Increased hydration matrix may also repel the external aggressive ions from the cover concrete. It is notable that even at a given time and the same concrete mix, the variation in the D was observed. It may be attributed to different environmental conditions, such as a degree of wave to the pier of the bridges, shade and wind, and moreover irregular location and shape of coarse aggregate may result in different chloride profiles, as chloride transport can be much influenced by the interfacial transition zone between cement matrix and aggregate, although the D is mainly affected by W/C [13], binder content [30] and binder type [15]. It was again observed that the C_S, was changed with the duration of exposure: the C_S increased in the form of a logarithm function with time for both OPC and GGBS concretes. It is not surprising at the increase in the C_S, since the tidal zone provides wet/dry cycles of seawater to the concrete bridge, so that chloride ions may be easily accumulated on the concrete surface. It is notable that at a given duration of exposure the C_S for GGBS concrete was usually higher than for OPC concrete, which seems attributed to different levels of chloride binding. The GGBS may impose the higher chloride binding capacity arising from higher level of aluminum oxide (Al_2O_3) [31]. Hence the surface of GGBS concrete is more capable of binding chlorides, compared to OPC concrete, at a given content of free chlorides, thereby leading to the higher total chlorides on the surface: in this study, the chloride concentration was expressed in total (i.e. acid soluble chloride).

To predict the rate of chloride ingress in a long term, the fit curves were extrapolated to 100 years. When the average value of the D and C_S at the youngest age (i.e. 0.65 years for OPC and 1.35 years for GGBS concretes, respectively) was taken as a control, their proportional development to exposure duration is described in Fig. 4. It is seen that a change in both the D and C_S is much affected by binder. The diffusivity of OPC concretes rapidly decreased for the first 20 years after exposure to a salt environment and then still decreased but at a lower rate up to about 75% of the initial D. For GGBS concretes, the D more rapidly decreased

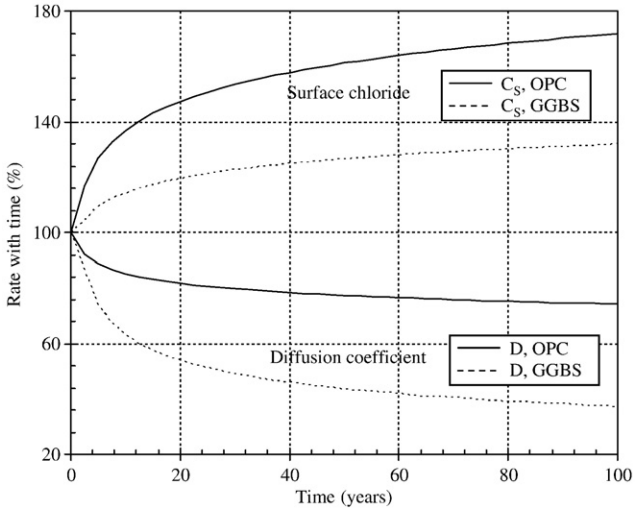

Fig. 4. Time dependent change in the apparent diffusion coefficient and surface chloride for OPC and GGBS concretes.

with time up to only 40% of the initial values. It may reflect the better long-term durability of GGBS concretes against chloride attack, in that the D at an early age for GGBS is, moreover, much lower than for OPC. The C_S for OPC highly increased up to by about 70%, compared to the initial value, while for GGBS by 30%.When it comes to the time dependency of chloride transport, the resistance to chloride attack depending on binder is of high complexity. GGBS concretes can be beneficent, since the D is lower and more rapidly decreases with time, and the C_S increases at a lower rate, compared to OPC concretes. However, the high level of initial C_S for GGBS concretes could partially offset the benefit of lower rate of chloride transport.

4.2. Chloride penetration

The chloride penetration by the time dependent/independent model (Eq. (11)) at 25, 50, 75 and 100 mm of the concrete cover is described in Fig. 5, for comparison (Eq. (1)). The chloride content was calculated with 2.5 years increments of the time interval. It is seen that the penetrated chloride ions calculated from the time dependent model was always higher than the time independent model. At an early age within 5–10 years, the penetration of chloride ions seemed not to be affected by time dependency of chloride transport; there was no particular difference between the time dependent and independent models. However, in a long term the penetrated chloride content for the time dependent model for OPC concretes was even higher than for the time independent model, in particular at the lower concrete cover. It may suggest that the influence of the increased C_S is dominant at chloride penetration, setting a higher concentration gradient of chloride ions on the concrete surface. However, as the cover depth increased, the difference of penetration of chlorides between two models decreased, since the increased C_S was less influencing and the D also governed the rate of chloride ingress.

For GGBS concretes, the penetration of chloride ions was varied with the concrete cover depth. At 25 mm, the penetrated chlorides obtained from the time dependent model was higher than the time independent model, and there was no difference between the models at 50 and 75 mm of the cover depth. At 100 mm, the time independent model produced higher level of chloride penetration. This can be explained by the lower rate of a build-up of the C_S, despite the greater C_S than for OPC concretes. At the lower cover depth, the C_S mainly drove chloride transport, and thus produced higher level of penetration for the time dependent model that considers a C_S build-up. However, at the deeper concrete, the affect of the increased C_S was relatively marginal and moreover the diffusivity decreased with time, eventually indicating the lower level of chloride penetration for the time dependent model, compared to the time independent model.

4.3. Chloride profile

The influence of the time dependency of chloride transport is described in Fig. 6, showing the different rate of chloride ingresses between time dependent and independent models. The chloride profiles

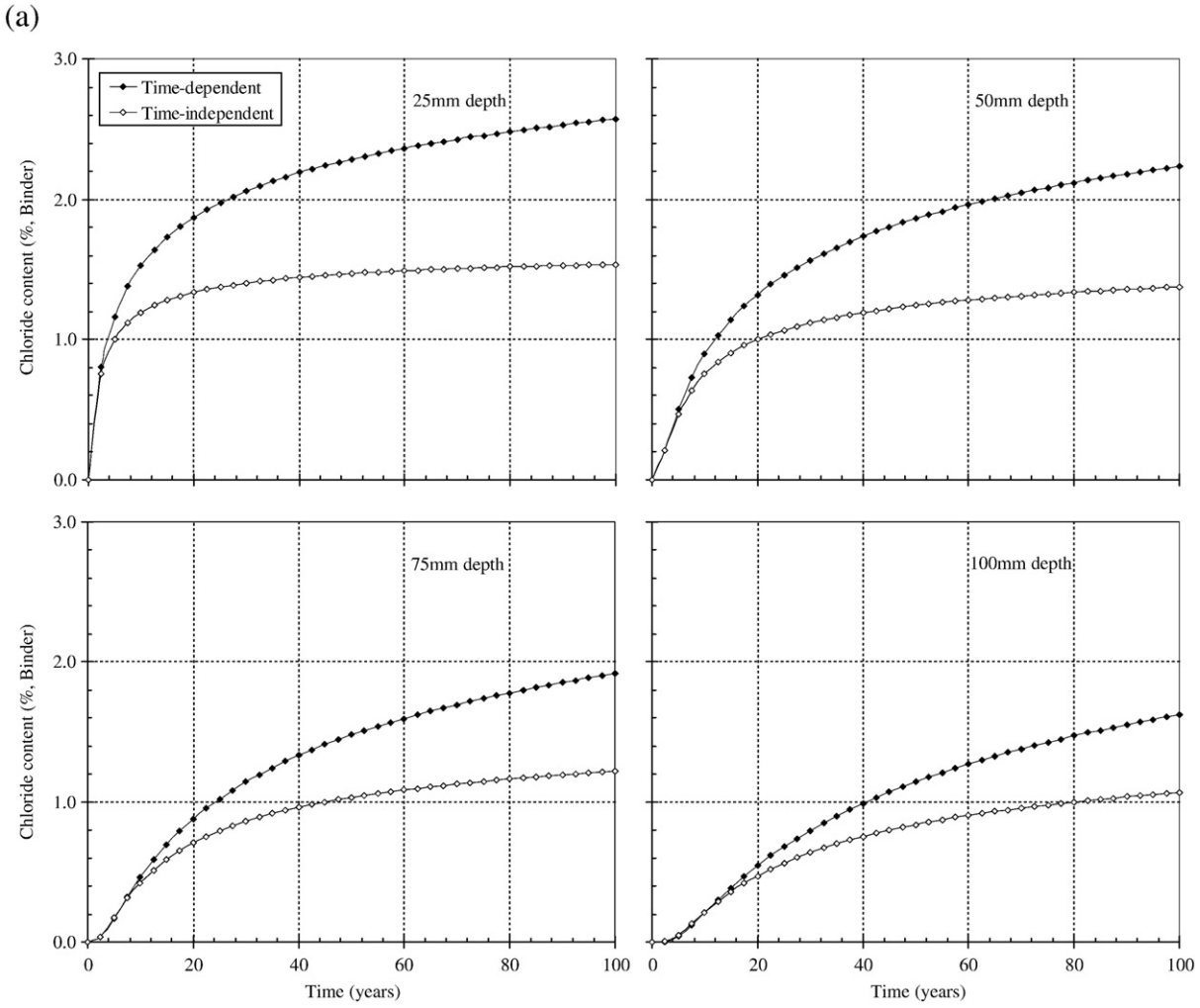

Fig. 5. Penetration of chloride ions at different concrete cover depth for (a) OPC and (b) GGBS concretes.

(b)

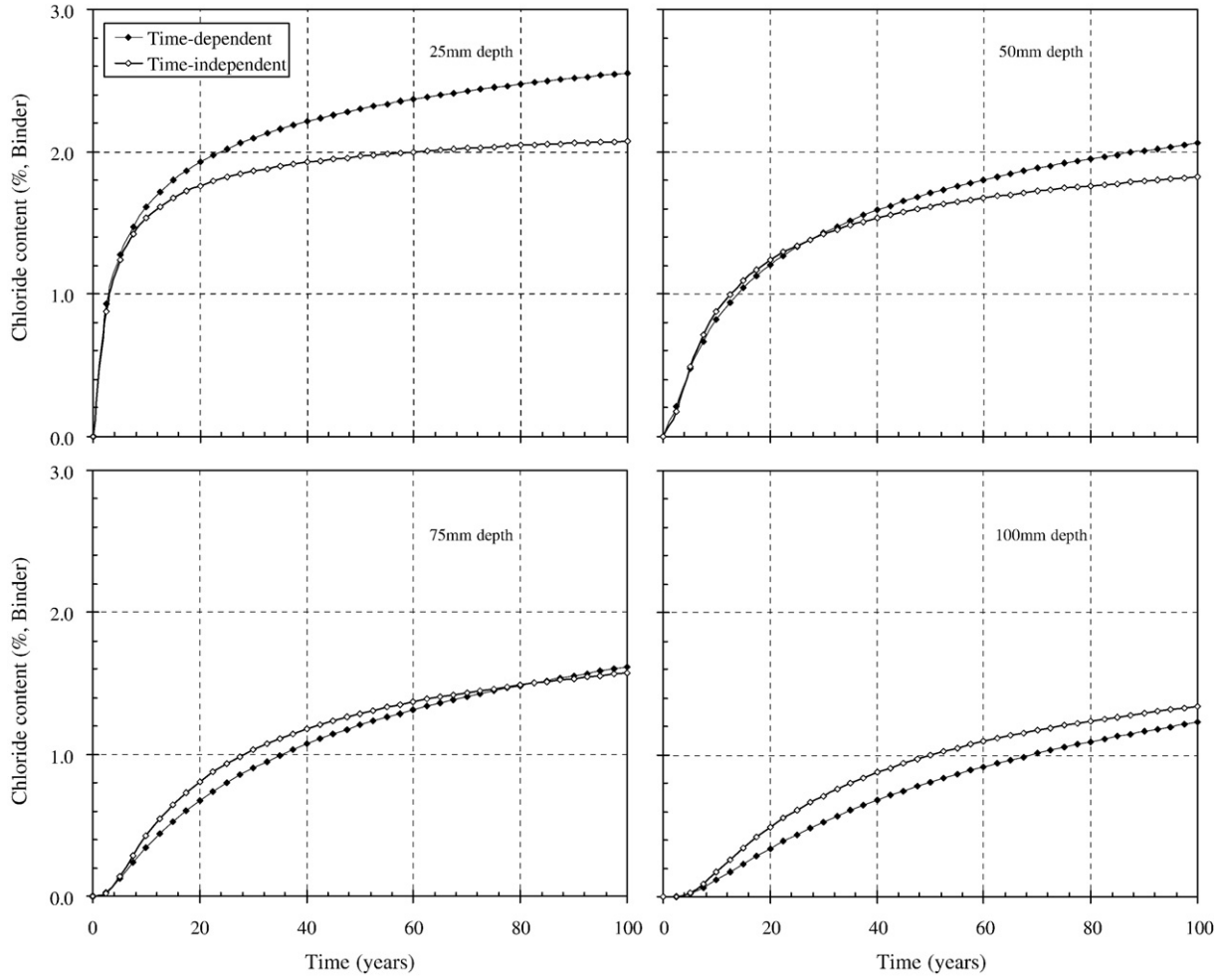

Fig. 5 (*continued*).

encompass a 100 mm of the concrete cover depth with increments of 2.5 mm from the surface concrete at 5, 20, 50 and 100 years. For OPC concretes, the chloride profiles calculated from the time dependent model were always higher than the time independent model and the chloride ingress increased with time at a much higher rate. It seems due to the higher C_S by a time dependent build-up of C_S. The concentration gradient of chloride ions on the surface concrete significantly increased with time and thus sustained the higher level of chloride ingress at all depths.

For GGBS concretes, the build-up rate of the C_S is relatively low, and hence the difference of chloride ingress on the surface concrete is not so significant, compared to OPC concrete. However, the dramatic decrease in the diffusivity seemed to affect the chloride profile. At 5 years, no particular difference in chloride ingress was observed except the C_S. At 20 and 50 years, for the time dependent model, the surface concrete produced the higher level of chloride ingress, but lower chloride content at deeper concrete beyond 50–60 mm of the cover concrete. Eventually, at 100 years, the chloride ingress from the time dependent model was higher than the time independent model within 85 mm of the cover concrete. It reflects the dominance of a significant fall in the diffusivity of GGBS concretes (Fig. 4). For the time dependent model, a build-up of the C_S is even more crucial in judging the chloride profile at an early age, but a reduction of the D with a combined effect of the increased C_S subsequently produced higher chlorides in the outer concrete and lower chlorides in the deeper concrete, compared to the time independent model.

4.4. Time to corrosion

The calculated time to corrosion for OPC and GGBS concretes with respect to the time dependency of chloride transport is depicted in Fig. 7, assuming the chloride threshold level for corrosion equates to 0.4% by weight of binder [9]. The concrete cover depth of up to 100 mm was considered with increments of 2.5 mm. For OPC concretes, the time dependent model produced the lowest level of the time to corrosion, presumably due to the highest development of the C_S with time and a relatively small decrease in the diffusivity. In contrast, for GGBS concretes, the time to corrosion calculated from the time dependent model was longer than that by the time independent model, since the development of hydration significantly decreased the diffusivity with time and a build-up of the C_S was relatively lower, compared to OPC concretes. Thus, the reduction of the D enhanced the time to corrosion over the increased C_S. When it comes to binder, GGBS concretes always produced the longer time to corrosion than OPC concretes. It may be due to the filler effect of GGBS, and thus its effect on the pore structure refinement and resistance to chloride transport may delay the onset of corrosion [32]. The time to corrosion calculated in this study was tried to compare to that for in-situ

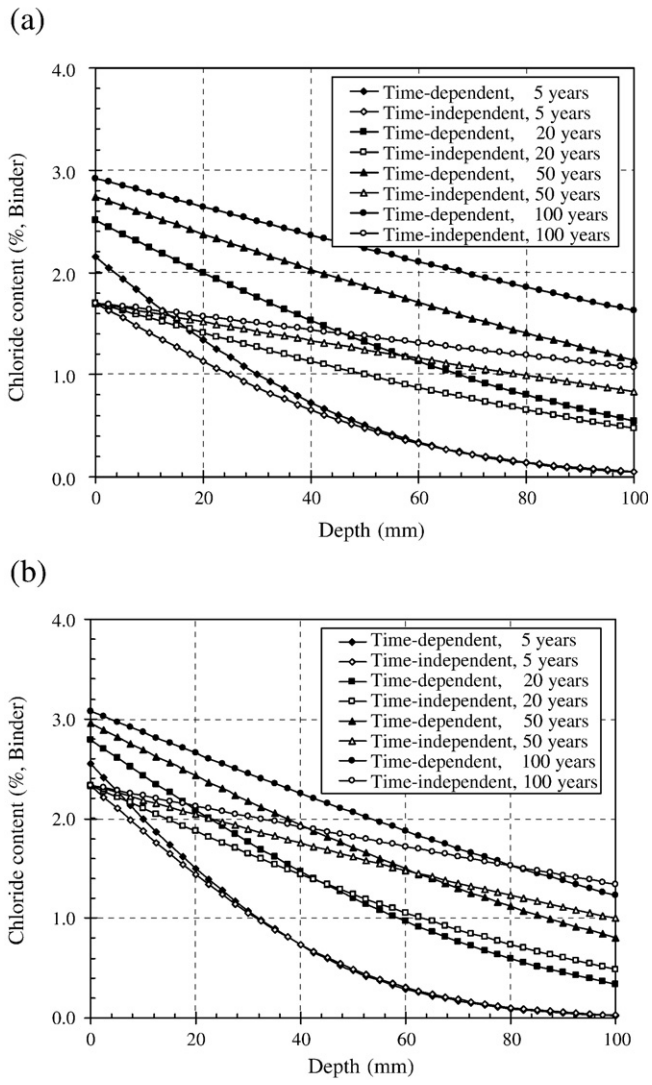

Fig. 6. Chloride profiles with time for (a) OPC concretes and (b) GGBS concretes.

structures, but the corrosion state has not been monitored for indicating the time to corrosion. Thus, a direct comparison for the accuracy of the calculation was not unfortunately performed.

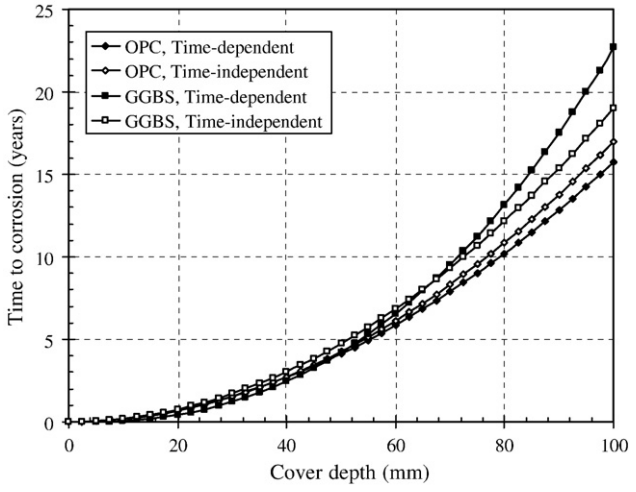

Fig. 7. Time to corrosion initiation of OPC and GGBS concretes.

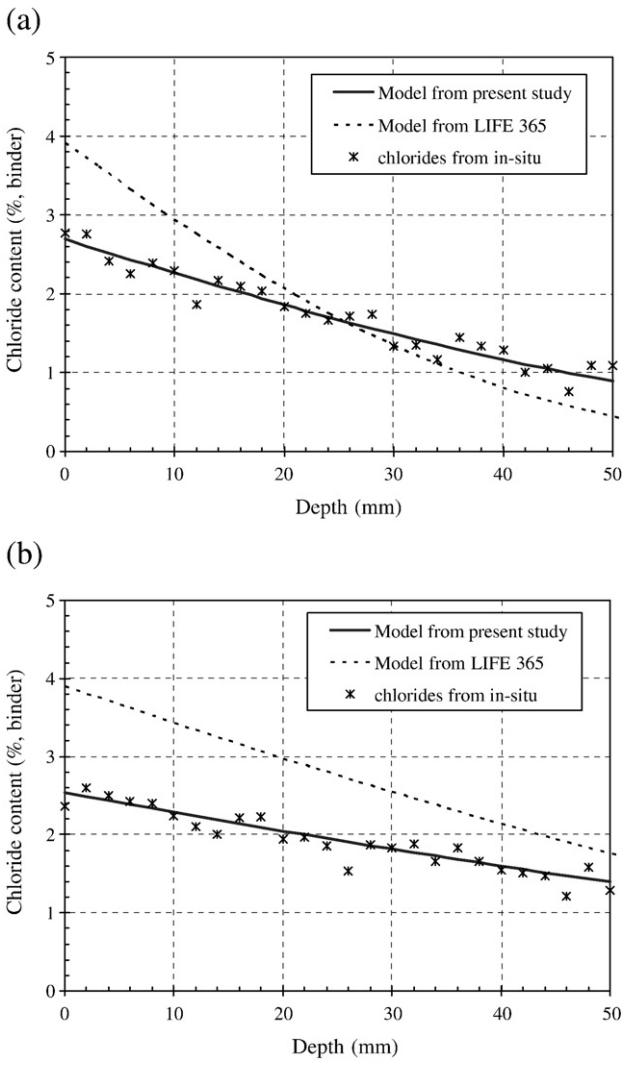

Fig. 8. Chloride profiles obtained from in-situ data and models in the present study and LIFE 365. (a) OPC concrete. (b) GGBS concrete.

5. Discussion

5.1. General (factors to chloride transport)

For chloride transport, aggregates usually have very low permeability and therefore have little impact on the permeation of chloride. Hence the rate of transport in a concrete is largely dependent on the characteristics of cement paste, in terms of the concrete pore structure, concrete mix proportion, curing and exposure conditions.

5.1.1. Pore structure

Hydrated cement paste contains several types of voids which have an important influence on its properties such as strength development, ionic transport and volume change in hardened concrete. The voids include gel pores, capillary pores and air voids. Gel pores are the smallest voids in concrete, ranging from 5 to 25 Å, and are too small to have an adverse effect on the ionic transport or strength of the concrete [19], while entrapped/entrained air voids, accounting for about 1.5% of the total volume of concrete, despite their large size, do not normally influence the transport properties as they are not connected with each other [33]. Only capillary pores are the most important when considering the ionic transport in concrete, as they are interconnected and filled with the pore solution. Their size ranges up to 3 to 5 μm in diameter. The rate of chloride transport via capillary pores is dependent on the volume fraction and

Table 3
The diffusion coefficient and surface chloride concentration calculated from diffusion models in the present study and LIFE 365.

	Exposure time (years)	Present study					LIFE 365				
		Initial value		Value at the given time			Initial value		Value at the given time		
		D (m^2/s)	C_S (%, binder)	D (m^2/s)	C_S (%, binder)	R^2	D (m^2/s)	C_S[a] (%, binder)	D (m^2/s)	C_S (%, binder)	R^2
OPC	22.54	6.74×10^{-12}	1.38	5.81×10^{-12}	2.54	0.88	6.74×10^{-12}	3.90	3.32×10^{-12}	3.90	–
GGBS	11.36	5.03×10^{-12}	2.01	3.99×10^{-12}	2.69	0.93	5.03×10^{-12}	3.91	1.50×10^{-12}	3.91	–

[a] The C_S for the LIFE 365 is set 0.8% to concrete weight and then converted to the percentage by binder weight.

connectivity of the pores, and can be determined from the W/C, cement content, cement fineness, cement type, use of replacement material and degree of hydration. For example, low W/C, good curing and replacement with pozzolanic materials will result in the capillary pores being blocked with gel and a reduced permeability to water-containing aggressive ions such as chlorides.

5.1.2. Concrete mix

It is well known that binder type and *W/B* significantly affects chloride transport, since the pore structure is differently formed, depending on concrete mix proportion. For example, pulverized fuel ash (PFA) or GGBS in concrete produces a dense cement matrix with fewer capillary pores due to the pozzolanic reaction [32]. Moreover, the particle size distribution in the finest range, which accounts for 100–1000 Å, for the other concrete constituents (i.e. filler effect) is more likely to reduce a chloride transport [21]. This study also showed from a survey of concrete bridges (i.e. OPC and GGBS concretes) exposed to a marine environment that the GGBS concrete always indicated much lower values of *D* than OPC one, by about 2–3 times, at a given time of exposure, when the exposure condition was similar. Hence, it is often said that a reduction of the *D* for PFA, GGBS and silica fume (SF) concretes generally arises from (1) a refinement of pore structure [21], or/and (2) the increased binding capacity [34,35]. The influence of W/B and binder content on the rate of chloride transport has been well addressed in the majority of previous studies. A literature review on chloride transport done by Song et al. [36] showed that an increase in the W/B about 20–25% resulted in a 1 order increase in the *D* irrespective of binder type for the similar exposure duration and external environment. The influence of cement or binder content on chloride transport was also previously ensured. Buenfeld and Okundi [30] showed, from chloride solution-exposure testing, that the higher binder content, at a given *W/B*, could increase chloride ion ingress in terms of the *D* and C_S, irrespective of binder type.

5.1.3. Hydration products

A proportion of chloride ions present in concrete is chemically bound, primarily by tricalcium aluminate (C_3A) to form Friedel's salt. Recent studies have modelled the influence of binding on the penetration of chloride [24,37]. Glass and Buenfeld [24] found that with increased chloride binding capacity, total chloride contents increase nearer the surface of the concrete, but decrease deeper in the concrete. An increase in the C_S is induced by the binding effect which allows the progressive build-up of higher total chloride content at increasing distances from the concrete surface. Chloride binding also reduces the content of free chloride within concrete and the concentration gradient at depth, because chloride binding removes chloride from the transport process [31]. It is notable that the content of bound chloride depends on the binding behaviour of cement matrix and the concentration of chloride source.

5.1.4. Curing

Curing methods and duration control the concrete quality including strength development, cement hydration and the rate of hydration, and durability of concrete. Bamforth [13], and Bamforth and Price [28] addressed the influence of curing methods on chloride transport and as a result, the *D* for OPC, 30% PFA, 70% GGBS and 8% SF concretes was not significantly affected by the curing method, while the C_S was varied with curing. It is seen again that the C_S was increased with time: the C_S ranged from 0.44 to 0.69% by weight of cement at 3 years of exposure, while the C_S increased up to 1.66–6.45% after an 8 year exposure.

5.1.5. Exposure condition

The level of chloride transport may be varied to a large degree by the location of structure, the degree of exposure to chloride environment and weathering condition with regard to temperature and humidity. Uji et al. [18] showed from a long-term monitoring from 23 to 58 years that the order of C_S with regard to the degree of vicinity of seawater is tidal > splash > atmospheric zone. The climate is also a crucial impact to the rate of chloride transport. Song et al. [36] compared the chloride transport of concrete from three different latitudes: in the UK, Japan and Venezuela. Then they found that concrete structures exposed to a tropical environment are more susceptible to chloride attack, and concluded that the tropical climate is better for chloride ions to move into concrete due to the high level of relative humidity, temperature and chloride concentration. The high temperature and humidity help chloride ions percolate concrete via absorption altogether with diffusion.

5.2. Time dependency of chloride transport

A reduction of the rate of chloride transport is ascribed to a development of cement hydration. Cement matrix usually completes 85–90% of the hydration within 28–56 days after casting. The rest of hydration takes place in a very long term, ranging from a couple of years to decades. When cement hydration proceeds, the hydration products expand twice of the volume and thus may occupy the capillary pore or block the interconnected network. Thus, the rate of chloride transport could significantly decrease with time. This effect was once modelled using a computational technique [38], but the results was less conclusive, since only the change of geometry in the capillary pore network (i.e. volume fraction) with time was taken into account. In fact, the rate of chloride transport is much affected by other factors including chemistry between chloride ions and cement matrix [33], and physical condition of the interfacial zone between cement paste and aggregate [39], which are also attributed to a chloride ions' mobility. Hence, it seems required to further investigate the time dependency of the rate of chloride transport, considering the complexity of physical and chemical change in cement matrix.

In this study, it was shown from a survey of concrete bridges in a marine environment that the *D* decreased and the C_S increased with the duration of exposure to seawater, assuming that chloride transport is restricted by only diffusion. According to the survey results, relations between the *D* and time, and the C_S and time were defined to model the time dependency of chloride transport, when concrete structure is exposed to the tidal/splash zone. As a result, the boundary condition for the model was set: the *D* decreases in the form of an exponential function to time until the first 30 years of the exposure, while the C_S increases in the form of logarithm function to time. It should be noted that most of previous models did not concern the characteristics of time dependent increase in the C_S, as direct contact of the cover concrete to seawater has been intuitively believed to form a chemical balance between cement matrix and chloride ions then to form a constant C_S [12,40]. Furthermore, a

decrease in the D with time has been overwhelmingly evaluated. For example, the age factor on D is determined for LIFE 365 as 0.43 [12], and for Duracrete as 0.6 [40], respectively, while the much lower values of 0.06 or 0.23 was more appropriate in describing the time dependency of chloride transport in the present study. Then, the accuracy in predicting the chloride profile was compared between the LIFE 365 and the present study. Fig. 8 gives the chloride profiles obtained from an in-situ autopsy with the curves modelled by the present study and the LIFE 365. For OPC concretes, the initial values of D and C_S at 1 year are set as 6.57×10^{-12} m^2/s, and 1.79% to the binder weight respectively and the reference chloride profile was from sample number 12 in Table 1. For GGBS concrete, the initial D and C_S were 5.39×10^{-12} m^2/s, and 2.29% to the binder weight respectively and the chloride profile from the in-situ was referred from sample number 14 in Table 2. The values of D and C_S obtained from the present study, the LIFE 365 and in-situ examination are compared in Table 3. It is evident that the model that the present study suggested better describes the chloride profile at 0–50 mm of the concrete cover for both OPC and GGBS concretes at 22.54 and 11.36 years respectively. The determinant coefficient to the modelled curves in the present study accounted for 0.88 and 0.93 for OPC and GGBS concretes, while the curves for the LIFE 365 did not well fit the chloride profile and thus the determinant coefficient was below zero. The inaccuracy of the LIFE 365 in predicting the chloride profile and transport may arise from the overestimation of the decrease in the D and a constant value of the C_S. In modelling the ingress of chloride ions, the LIFE 365 assumes that the C_S keeps a constant value, as being equivalent to 0.8% to the weight of concrete (i.e. 3.90 and 3.91% for OPC and GGBS concretes in this study), while the C_S obtained from the in-situ ranged 2.36 and 2.54% to the binder weight for OPC and GGBS concretes respectively. In the present study, the growth model for the time dependent C_S indicated 2.54 and 2.69% at the given duration of exposure for OPC and GGBS concretes respectively, being mostly equated to the values obtained from an in-situ examination. Furthermore, the D predicted in the LIFE 365 was much lower than the in-situ value, due to an overestimation of the decreasing rate of chloride transport. For example, the D for OPC concretes calculated by the LIFE 365 model was 3.32×10^{-12} m^2/s at 22.54 years, while the present study predicted the D as 5.81×10^{-12} m^2/s at the equated time of exposure, which is closer to the value of the D obtained from the in-situ. Consequently it seems that the previous model (i.e. LIFE 365) must contain the following boundary conditions: (1) an increase in the C_S with time even at the tidal/splash zone and (2) lower rate of decreasing D, based on the data from real structures.

A reduction of ionic diffusivity through concrete with time is beneficial in delaying the onset of chloride-induced corrosion and thus enhancing the corrosion free life of structures. However, a build-up of the C_S may mitigate the benefit of decreased diffusivity, or produce a higher ingress of chloride ions. It was seen in this study that a combination of a build-up of the C_S and decreased D for GGBS concretes produced a similar level of the chloride ingresses, compared to the model neglecting the time dependency of chloride transport, while for OPC concrete produced a higher chloride profile. Hence, to maximise the beneficial effect of decreased diffusivity, it is required to reduce or at least sustain the C_S.

The present study showed the benefits of GGBS concretes against chloride transport from a lower diffusivity at an early age and its significant reduction with time, compared to OPC concretes. A rapid decrease in the D for GGBS concretes may be attributed to their hydration rate and the original pore volume. GGBS paste hydrates at a lower rate and thus it takes longer to meet the hydration degree of OPC paste, termed a "latent hydration," which may be responsible for the low-rated strength development. However, the latent hydration once proceeds to refine the pore structure of GGBS paste and to form a lower level of the capillary pore connectivity, it leads to a significant decrease in the rate of chloride transport. Moreover, the original porosity is also lower than for OPC concretes, as the finely grained GGBS fills up the voids/pores in cement matrix [13]. Moreover, GGBS is very resistant to chloride-induced corrosion and guarantee a low corrosion risk. The majority of previous studies showed the highly inhibitive nature of GGBS concretes in terms of the chloride threshold level for corrosion [32,41], and to corrosion propagation [35,42]. These benefits have been led to a wide use of GGBS concretes to in-situ, in particular located in a marine or salt environment (e.g. deicing salt).

6. Conclusion

The present study surveyed 11 bridges exposed to a seawater environment in assessing their resistance to chloride transport through concretes in terms of diffusion. The obtained results from the survey of in-situ were used to model for a long-term prediction of chloride profile, considering the time dependency of chloride transport. The conclusion is as follows.

(1) The D of chloride ions in concrete obtained from in-situ marine environments decreased in the form of an exponential function to time, irrespective of binder type, and the C_S increased in the form of a logarithm function to time. This relation was used to predict the chloride ingress in concrete structures exposed to the tidal/splash zone in a long term.
(2) For OPC concrete, the time dependent model indicated the higher ingresses of chloride ions than the time independent model at a given time of exposure, because of the higher C_S, thereby leading to a shorter time to corrosion at a given chloride threshold level for corrosion. However, for GGBS concrete, similar range of chloride ingress was predicted between the time dependent and independent model. This may arise from the more rapid reduction of the D for GGBS concretes which imposes a further latent hydration and thus densifies the concrete pore structure.
(3) The accuracy of the present study and a well know conventional model of the LIFE 365 was compared with chloride profiles obtained from an in-situ examination. Consequently, the model that the present study proposed well rendered the ingresses of chlorides, while the LIFE 365 showed a poor prediction of the chloride profile, due to a constant value of C_S and overestimation of decreasing rate of D.

Acknowledgement

The authors would like to thank the financial support from the project on Standardization of Construction Specifications and Design Criteria based on the Performance and Center for Concrete Corea, Republic of Korea.

Appendix A. Supplementary data

Supplementary data associated with this article can be found, in the online version, at doi:10.1016/j.cemconres.2009.09.023.

References

[1] C.L. Page, Mechanism of corrosion protection in reinforced concrete marine structure, Nature 256 (1975) 514–515.
[2] C.L. Page, K.W.J. Treadaway, Aspects of the electrochemistry of steel in concrete, Nature 297 (1982) 109–115.
[3] K.C. Clear, Effectiveness of epoxy-coated reinforcing steel, Concr. Int. 14 (1992) 58–64.
[4] T.H. Hong, S.H. Chung, S.W. Han, S.Y. Lee, Service life estimation of concrete bridge decks, KSCE J. Civil Eng. 10 (2006) 233–241.
[5] C. Jaegermann, Effects of water–cement ratio and curing on chloride penetration into concrete exposed to a Mediterranean Sea climate, ACI Mater. J. 87 (1990) 333–339.
[6] K.C. Liam, S.K. Roy, D.O. Northwood, Chloride ingress measurements and corrosion potential mapping study of a 24 year old reinforced concrete jetty structure in a tropical marine environment, Mag. Concr. Res. 44 (1982) 205–215.

[7] P.D. Cady, R.E. Weyer, Prediction service life of concrete bridge decks subjected to reinforcement corrosion, in: V. Chaker (Ed.), Corrosion Forms and Control for Infrastructure, ASTM STP, vol. 1137, 1992, pp. 302–324.
[8] ACI Committee 222, Corrosion of metals in concrete, Manual of Concrete Practice, Part 3, American Concrete Institute, Detroit USA (1994).
[9] British Standard 8110, Structural use of concrete—code of practice for design and construction, Part 1, British Standards Institute, London UK (1985).
[10] M. Collepardi, A. Marcialis, R. Turriziani, Penetration of chloride ions into cement pastes and concrete, J. Am. Ceram. Soc. 55 (1972) 534–535.
[11] P.D. Cady, R.E. Weyers, Chloride penetration and the deterioration of concrete bridge decks, Cem. Concr. Agg. 5 (1983) 81–87.
[12] M.D.A. Thomas, E.C. Bentz, Life-365 manual, released with program by Master Builders (2000).
[13] P.B. Bamforth, The derivation of input data for modelling chloride ingress from eight-years UK coastal exposure trials, Mag. Concr. Res. 51 (1999) 87–96.
[14] R.E. Weyers, M.G. Fitch, E.P. Larsen, I. Al-Qadi, W.P. Chamberlin, P.C. Hoffman, Concrete bridge protection and rehabilitation: chemical and physical techniques, service life estimates, Strategic Highway Research Program, National Research Council, Washington DC (1994).
[15] P.S. Mangot, B.T. Molloy, Prediction of long term chloride concentration in concrete, Mat. Struct. 27 (170) (1994) 338–346.
[16] S.L. Amey, D.A. Johnson, M.A. Miltenberger, H. Farzam, Predicting the service life of concrete marine structures: an environment methodology, ACI Struct. J. 95 (1998) 205–214.
[17] M.K. Kassir, M. Ghosn, Chloride-induced corrosion of reinforced concrete bridge decks, Cem. Concr. Res. 32 (2002) 139–143.
[18] K. Uji, Y. Matsuoka, T. Maruya, Formulation of an equation for surface chloride content of concrete due to permeation of chloride, corrosion of reinforcement in concrete, Elsevier Applied Science (1990) 258–267.
[19] P.K. Mehta, P.J.M. Monteiro, Concrete structure, properties and materials, 2nd ednPrentice Hall, 1993.
[20] Japan Society of Civil Engineers (JSCE). Standard specification for durability of concrete, Concrete Library, in Japanese (2002) 83–88.
[21] S.E. Hussain, S. Rasheeduzafar, Corrosion resistance performance of fly ash blended cement concrete, ACI Mater. J. 91 (1994) 264–273.
[22] M.D.A. Thomas, P.B. Bamforth, Modelling chloride diffusion in concrete effect of fly ash and slag, Cem. Concr. Res. 29 (1999) 487–495.
[23] E.C. Bentz, C.M. Evans, M.D.A. Thomas, Chloride diffusion modelling for marine exposed concretes, in: C.L. Page, P.B. Bamforth, J.W. Figg (Eds.), Corrosion of Reinforcement in Concrete Construction, Cambridge, UK, 1996, pp. 136–145.
[24] G.K. Glass, N.R. Buenfeld, The influence of chloride binding on the chloride induced corrosion risk in reinforced concrete, Corros. Sci. 42 (2000) 329–344.
[25] W. Feller, An introduction to probability theory and its applications, John Wiley, New York, 1971.
[26] H.S. Shim, Corner effect on chloride ion diffusion in rectangular concrete media, KSCE J. Civil Eng. 6 (2002) 19–24.
[27] H.-W. Song, S.-W. Pack, J.S. Moon, Durability evaluation of concrete structures exposed to marine environment focusing on a chloride build-up on concrete surface, Proceedings of the International Workshop on Life Cycle Management of Coastal Concrete Structures, Nagaoka Japan (2006) 1–9.
[28] P.B. Bamforth, W.F. Price, Factors influencing chloride ingress into marine structures, Proceeding of conference on Concrete 2000. Economic and Durable Construction through Excellence, E & FN Spon, London UK, 1993, pp. 1105–1118.
[29] H.S. Carslaw, J.C. Jaeger, Conduction of heat in solids, The Clarendon Press (2). Oxford (1959).
[30] N.R. Buenfeld, E. Okundy, Effect of cement content on transport in concrete, Mag. Concr. Res. 50 (1998) 339–351.
[31] H.-W. Song, C.-H. Lee, K.Y. Ann, Prediction of chloride profile considering binding of chlorides in cement matrix, International Corrosion Engineering Conference, Seoul Korea, 2007.
[32] P. Schiessl, W. Breit, Local repair measures at concrete structures damaged by reinforcement corrosion, in: C.L. Page, P.B. Bamforth, J.W. Figg (Eds.), Corrosion of Reinforcement in Concrete Construction, Cambridge, UK, 1996, pp. 525–534.
[33] G.K. Glass, N.R. Buenfeld, Chloride-induced corrosion of steel in concrete, Prog. Struc. Eng. Mater. (2000) 448–458.
[34] R.K. Dhir, M.A.K. El-Mohr, T.D. Dyer, Chloride binding in GGBS concrete, Cem. Concr. Res. 26 (1996) 1767–1773.
[35] R. Luo, Y. Cai, C. Wang, X. Huang, Study of chloride binding and diffusion in GGBS concrete, Cem. Concr. Res. 33 (2003) 1–7.
[36] H.-W. Song, C.-H. Lee, K.Y. Ann, Factors influencing chloride transport in concrete structures exposed to marine environments, Cem. Concr. Compos. 30 (2008) 113–121.
[37] B. Martin-Perez, H. Zibara, R.D. Hooton, M.D.A. Thomas, A study of the effect of chloride binding on service life predictions, Cem. Concr. Res. 30 (2000) 1215–1223.
[38] E.J. Garboczi, D.P. Bentz, Computer simulation of the diffusivity of cement-based materials, J. Mater. Sci. 27 (1992) 208–392.
[39] C. Famy, K.L. Scrivener, A.K. Crumbie, What causes differences of C–S–H gel grey levels in backscattered electron images? Cem. Concr. Res. 32 (2002) 1465–1471.
[40] DuraCrete, Final Technical Report—probabilistic performance based durability design of concrete structures. Document BE95-1347/R17, European Brite-Euram Programme, (2000).
[41] B.H. Oh, S.Y. Jang, Y.S. Shin, Experimental investigation of the threshold chloride concentration for corrosion initiation in reinforced concrete structures, Mag. Concr. Res. 55 (2003) 117–124.
[42] C.L. Page, N.R. Short, W.R. Holden, The influence of different cements on chloride-induced corrosion of reinforcing steel, Cem. Concr. Res. 16 (1986) 79–86.